Seasonal variations in sea level induced by continental water mass: First results from GRACE

B. Wouters,[1] R. E. M. Riva,[2] D. A. Lavallée,[2] and J. L. Bamber[3]

Received 9 November 2010; revised 15 November 2010; accepted 27 December 2010; published 4 February 2011.

[1] Variations in the Earth's water cycle are commonly quantified by their effect on global mean sea-level. However, the interaction between passive adjustment of the ocean to changes in gravitational attraction due to mass redistribution, the related deformation of the solid Earth and disturbances in the Earth's rotation vector will yield a distribution that is more complicated than a uniform rise or fall of the ocean's surface. In this study, we present the first estimates of seasonal changes in passive sea-level (which we define as the height difference between the sea surface at rest and ocean floor, excluding steric and dynamical effects) based on direct observations of surface mass redistribution, made by the Gravity Recovery and Climate Experiment (GRACE) between 2003 and 2010. We show that this "selfgravitation-effect" causes seasonal variations of the sea-level of up to 1 cm – comparable to the amplitude of the long-period tides – and that inclusion in numerical ocean models results in a better agreement between observed and modelled ocean bottom pressure variations, particularly in coastal zones. **Citation:** Wouters, B., R. E. M. Riva, D. A. Lavallée, and J. L. Bamber (2011), Seasonal variations in sea level induced by continental water mass: First results from GRACE, *Geophys. Res. Lett.*, *38*, L03303, doi:10.1029/2010GL046128.

1. Introduction

[2] Regional sea-level is affected by multiple forcing mechanisms, such as ocean dynamics and the interaction with the overlying atmosphere. Even in absence of such forcings, the ocean will adapt passively to changes in the gravitational potential field, of which the luni-solar tidal effects are an exemplary manifestation. A less well known forcing is the gravitational pull exerted by continental surface masses, which equally causes variations in the geopotential and subsequent deformation of the ocean floor. The theory behind this was first described more than 120 years ago, by *Woodward* [1888] and was later extended by *Farrell and Clark* [1976]. Their "sea-level equation" describes the joint response of an equilibrium ocean and the solid earth to changes in surface mass loading and was widely adopted by the solid earth community, where it is used to constrain, e.g., the Earth's glacial history. Other studies attempted to match the distinct spatial patterns in sea-level associated with the mass changes in the ice sheets and mountain glaciers (the so-called "fingerprints") to tide-gauge records to estimate their respective 20th-century melting rates [*Mitrovica et al.*, 2001].

[3] Aforementioned studies focused on centennial to millenial trends in relative sea level. However, similar variations can be expected on shorter time scales as well due to the seasonal redistribution of water on the continents [*Clarke et al.*, 2005]. Since the advent of satellite observations, numerous studies have described the annual exchange of water mass between continents and ocean, with an amplitude in the order of 8–10 mm and a peak in September–October [e.g, *Chambers et al.*, 2004]. These studies typically present global mean figures, suggesting that the water load distributes as a uniform layer in the ocean. Recently, *Tamisiea et al.* [2010] used the output of numerical geohysical models to obtain a more detailed picture of the annual cycle and showed that regionally passive sea level may deviate by up to 80% from the global mean. However, current hydrological models lack a number of first-order components of the hydrological cycle, such as water storage in the groundwater layer, open lakes and the cryosphere and are known to poorly represent storage changes in certain regions, such as areas permanently covered with snow [e.g., *Rodell and Houser*, 2004]. These components constitute a significant quantity of the total signal, such model deficiencies will therefore result in a bias in the modelled passive sea level cycle.

[4] The GRACE twin-satellite mission allow the retrieval of changes in the integrated surface mass distribution on the Earth at a resolution of a few 100 km at quasi-monthly intervals [*Tapley et al.*, 2004]. The observations include all components of the hydrological cycle and given their global coverage of continental redistribution on land – the input data required for solving the sea-level equation – they offer an excellent tool to realistically derive changes in passive sea-level. Here, we use the GRACE observations to derive the first estimates of the annual, hydrology-induced, cycle in passive sea level based on direct observations.

2. Data and Method

[5] As an input for the sea level equation, we use 80 monthly GRACE solutions between March 2003 and February 2010, released by the Center for Space Research (CSR RL04). We complement the GRACE observations with degree 1 coefficients (which are not observed by GRACE) based on a combination of ocean model output and GRACE data over land [*Swenson et al.*, 2008]. The original C_{20} coefficients were replaced by values derived from satellite laser ranging (R. Eanes, personal communication, 2008). At shorter wavelengths, the GRACE data are

[1]Netherlands Royal Meteorological Institute, De Bilt, Netherlands.
[2]Delft Institute of Earth Observation and Space Systems, Delft University of Technology, Delft, Netherlands.
[3]Bristol Glaciology Centre, School of Geographical Science, Bristol, UK.

0094-8276/11/2010GL046128

contaminated by correlated noise. Therefore, the coefficients were post-processed using an empirical orthogonal function approach [*Wouters and Schrama*, 2007]. The advantage of EOF filtering is that no further spatial smoothing is required, which would lead to signal attenuation and leakage between hydrological signals in adjacent regions.

[6] The sea level equation describes how dynamic load components (continental water, ocean and atmosphere) combine with passive sea level to give the observed geoid. Traditionally the dynamic load components come from hydrologic, atmospheric and ocean models [*Clarke et al.*, 2005; *Tamisiea et al.*, 2010]. With GRACE the situation is different since we have the observed geoid itself rather than the dynamic load components. Strictly speaking this means that we must solve the sea level equation to obtain the separate dynamic components before estimating the passive sea level due to any individual component. This approach is taken by *Riva et al.* [2010] in their study of trends in present-day passive sea level, with the assumption of a passive ocean. On seasonal time scales, a substantial part of the ocean mass redistribution is wind-driven and this assumption might not longer hold. Here we clip atmosphere corrected GRACE over land using a smoothed landmask that gradually evolves from unity over the continents to zero over the oceans, within a distance of 300 km [*Chambers et al.*, 2007] and use this as an approximation of the dynamic continental water load. We then proceed to calculate its passive sea level fingerprint (see auxiliary material).[1] Errors due to the selected method and residual noise in the GRACE data are captured in our error analysis (section 3).

3. Error Analysis

[7] The GRACE observations have a limited resolution, with a maximum spherical degree $l = 60$ for the CSR RL04 solutions (~333 kilometers). Hence, small-scale signals may not be fully detected by the GRACE satellites. Furthermore, as a consequence of the finite resolution and the smoothed landmask, hydrological signals in certain coastal areas may be weakened, or, conversely, mass variations in coastal shelf regions may be misinterpreted as occurring over land. Both factors will lead to divergence from the 'true' solution during the iterative solving of the sea-level equation, since the loading signals over land and oceans are not properly represented. Moreover, the post-processing procedure may affect the recovery of the surface water mass redistribution on land.

[8] We address these issues by using a set of synthetic maps of monthly mass anomalies as an input for the sea level equation. To this end, the output of the Global Land Data Assimilation System (GLDAS/Noah) [*Rodell et al.*, 2004] is combined with ocean bottom pressure (OBP) variations from the barotropic ECCO (Estimating the Circulation and Climate of the Ocean) model [*Fukumori et al.*, 1999]. The combined fields are converted to spherical harmonics and reconciled with the GRACE processing standards: the spherical harmonics are cut off at degree/order 60 and the post-processing procedure is applied to the coefficients; subsequently, the smoothed land function is used to isolate the land mass contributions, which are then used as input for the sea level equation. In a second run, used as a baseline for validation, we use the synthetic data at its highest resolution (max. spectral degree of $l = 512$ in the sea level equation), omit the EOF filtering and apply an exact landmask.

[9] Passive sea level estimated from both runs agrees well in shape and no systematic differences are observed. For the majority of the ocean (Figure S1), the values based on the GRACE-like data are within 5% of the values obtained from the validation run. Along some irregular coastlines, this value increases to ≈10%. The limited spatial resolution and the non-exact land mask only become a limiting factor in some regions, such as around the peninsula of Kamchatka (24% difference), where the relatively strong but small-scale hydrological signal in the GLDAS model cannot be fully captured, and in some coastal shallow water regions, e.g., the Gulf of Carpentaria (17%), where the large OBP variability is misinterpreted as occurring over land, due to the non-discrete land/ocean mask. The global mean amplitude of the annual cycle is slightly reduced by 0.2 mm, which we include in our error bars.

[10] A second source of uncertainty lies in the noise remaining after filtering in the GRACE solutions. The effect on our estimates of passive sea level was estimated using a Monte Carlo approach. The empirical errors spectrum [*Wahr et al.*, 2006] was used to create a set of pseudo-solutions by multiplying the standard deviation of each error coefficient with a normally distributed random number. These pseudo-solutions were then used as input for the sea level equation. The resulting passive sea level fields were used to create a large set of time series ($n = 1000$) with a length equal to the GRACE observation period. Finally, our error bars for the GRACE errors are based on the 2-σ range of this ensemble of amplitudes, normalized by the global mean amplitude obtained from the GRACE time series, and are in the order of 3–4% along the coast reducing to 1–2% in the open ocean (Figure S2).

[11] To test the robustness of the obtained relative sea level variations, we repeat our analysis for a second set of GRACE solution, provided by GeoForschungsZentrum Potsdam (RL04) and add the difference quadratically to the above two error estimates.

4. Results

[12] Figure 1a shows the annual variations in passive sea-level as a result of self-gravitation effects based on the CSR GRACE data, i.e., the sum of geoid changes and the radial displacement of the solid earth, induced by variations in continental mass loading (see Figure S3 for GFZ results). The global mean eustatic cycle, i.e., the total amount of water exchanged between continents and ocean, equals 9.4 ± .6 mm equivalent water level. Overall, the passive sea-level is characterized by long-wavelength patterns, with opposing deviations from the global mean in the two hemispheres. The Northern Hemisphere shows annual amplitudes below the global mean, due to the fact that water storage on the northern continents reaches a maximum mid-March (Figure 2), causing an enhanced gravitational attraction. This maximum is about 180° out-of-phase with the globally averaged (eustatic) cycle of ocean water content (peaking early October, day of year 280 ± 6), resulting in a reduced amplitude of the sum of the two components. In the Southern Hemisphere, the amplitude is consequently

[1] Auxiliary materials are available in the HTML. doi:10.1029/2010GL046128.

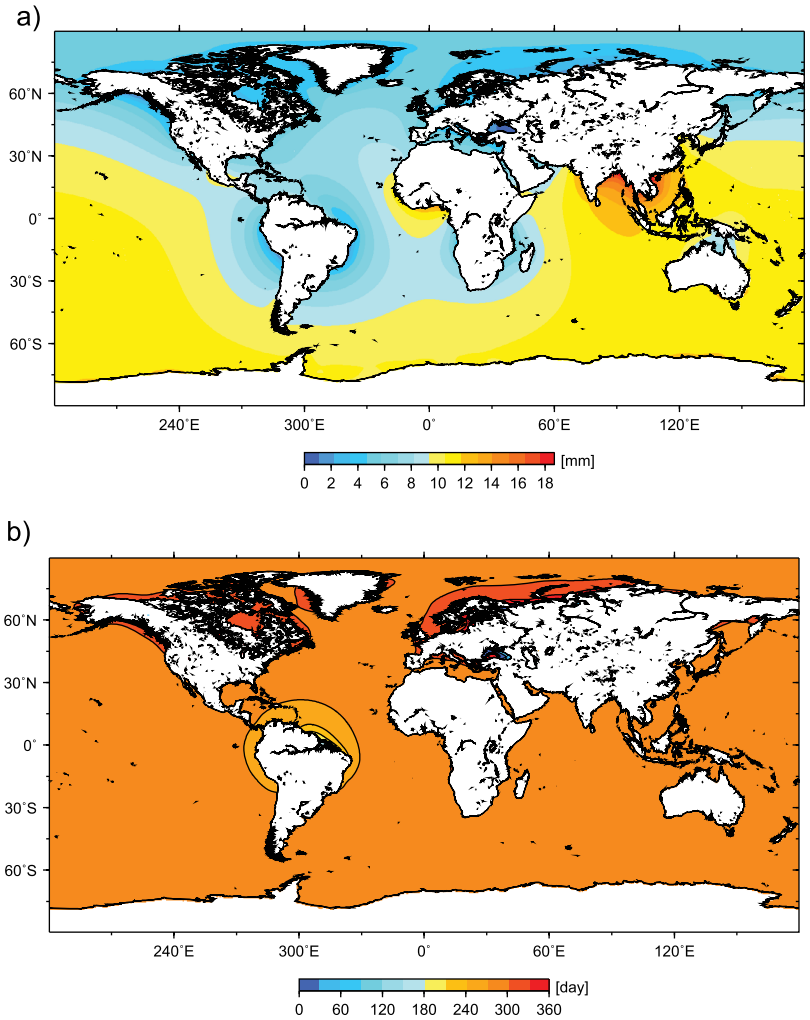

Figure 1. (a) Annual amplitude of the passive sea-level caused by the combined gravitational and radial displacement effects. The global eustatic annual amplitude is 9.4 ± 0.6 mm equivalent water level, peaking on day-of-year 280 ± 6. (b) phase of annual passive sea-level as day-of-year of the maximum relative to 1 January. Contour lines every 30 days.

generally larger than the global mean, except for the regions around the major hydrological basins, such as the Amazon basin or the Congo/Zambezi basin, where a similar reasoning applies. Maximum amplitudes are found around the major hydrological systems in the Northern subtropics, e.g., the Ganges–Brahmaputra or the Volta–Niger basins, where the peak in gravitational pull of terrestrial water storage (early October) coincides with the maximum in eustatic sea-level, resulting in an amplified signal.

[13] Maximum annual variability is found in the Bay of Bengal, where selfgravitation effects enhance the annual amplitudes to 17 ± 1.3 mm, or 216 ± 13% of the global mean. The smallest signal is found off the coasts of Alaska and British Columbia, with values as small as 1.1 ± 0.6 mm, only 14 ± 6% of the eustatic value. The phase of the annual passive sea-level (Figure 1b) is fairly homogeneous over the ocean, peaking in October, except around the Amazon basin, where the strong hydrological cycle introduces a bias of up to four months.

[14] On a basin scale, the Pacific Ocean shows an amplitude of 105% of the global eustatic mean, with most positive

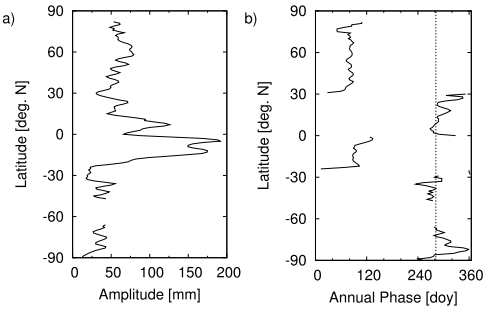

Figure 2. (a) Zonally averaged annual amplitude of continental water distribution anomalies expressed in mm equivalent water level and (b) day of maximum of the continental water storage from GRACE observations relative to 1 Jan. The dashed line shows the phase of the global mean eustatic sea-level. Continental water distribution anomalies in phase with the latter will result in a regionally amplified cycle of the passive sea-level due to the selfgravitation effects.

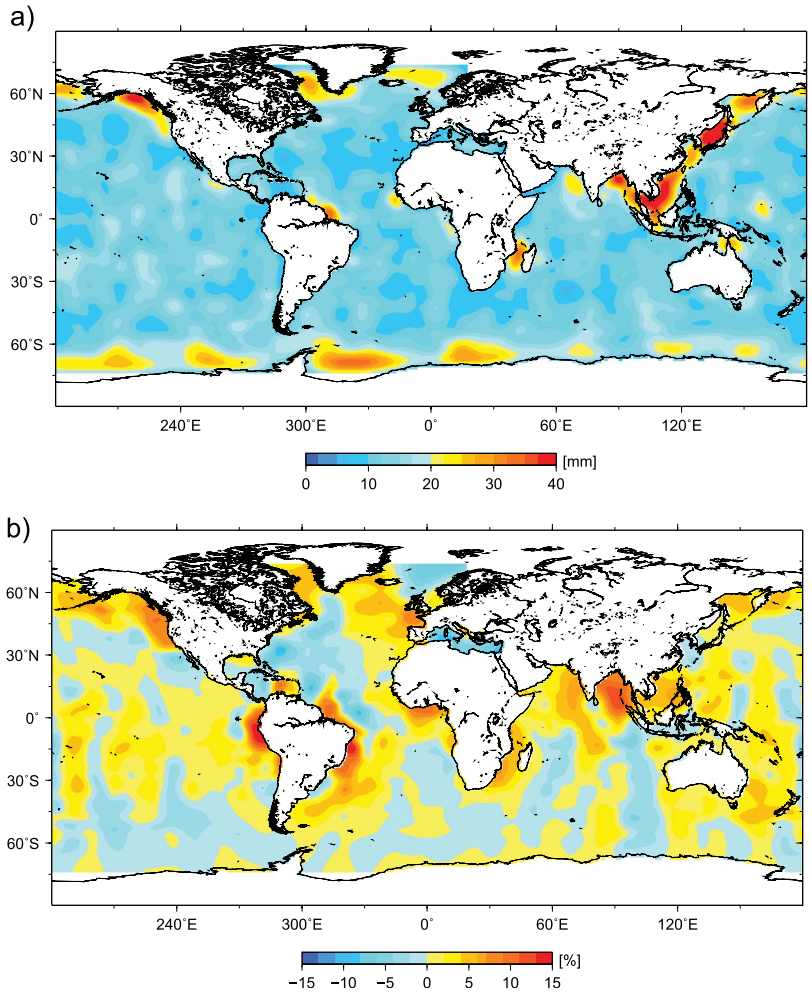

Figure 3. (a) Variance of the seasonal residuals of the GRACE observations and OBP from the ECCO model, expressed in mm water equivalent, and (b) reduction of the variance, divided by total variance in Figure 3a, after including effects on self-gravitation to the ECCO model.

values in the South (108% vs. 101% for the Northern Hemisphere). Slightly larger values are found in the Indian Ocean (111%). Below-average values are obtained in the Atlantic (88% with 91% South vs. 85% North Atlantic) and in the Arctic ocean (53%). Overall, 55% of the ocean experiences an annual cycle larger than the global average.

5. Validation With the ECCO Model

[15] Current numerical ocean models do not include the effects of selfgravitation as described in this article. Including these effects should therefore result in an improved reconciliation of model output and observational data. In the following, this hypothesis is tested by comparing OBP variations obtained from the GRACE data to the output of the ECCO model, with and without the selfgravitation effects included. For consistency, the monthly ECCO grids were first converted to spherical harmonics up to degree 60 and then transformed back to spatial grids. Since the GRACE data are considerably more contaminated by noise over the ocean than over land, both data sets are smoothed with a Gaussian radius of 350 km, after masking out land. High-frequency ocean mass variations, removed during processing of the raw GRACE data in order to prevent aliasing, were added back to the GRACE fields.

[16] The ECCO model uses the Boussinesq approach, conserving volume rather than mass. Therefore, before comparing to the GRACE observations, the global mean bottom pressure is subtracted from every grid point in the monthly ECCO grids. Next, the monthly mean ocean mass obtained from the GRACE observations is added to the ECCO fields as a uniform layer. The differences between the annual cycle in the GRACE observations and ECCO simulations are then computed and the variance of the seasonal residuals determined (Figure 3a). Largest residuals (~40 mm) are found in the marginal East China Sea, where the ECCO model shows strong OBP variability which is not observed by GRACE. The smallest residuals are found in the South Indian and have a variance of ~5 mm equivalent water height, which we take as an (admittedly optimistic) error estimate for the GRACE observations over the oceans at seasonal time-scales.

[17] The procedure is repeated, but now also GRACE-derived regional variations in OBP as a result of the hydrology-induced selfgravitation effects are added to the ECCO fields. Note that the resulting fields do not include direct GRACE observations over the oceans, allowing an independent comparison. The change in variance, scaled by

the original variance, is depicted in Figure 3b. The results of the test appear to be inconclusive for most of the open ocean, where differences are within a few percents of the original variance. Deviations of the annual passive sea level from the eustatic mean sea level are in the order of 10–20 % in these regions (compare Figure 1a), which translates to 1–2 mm in equivalent water height, below the noise level of the GRACE observations mentioned above. However, in regions where the selfgravitational effects exceed the minimal GRACE error – e.g., around the Amazon and Ganges basins and off the coast of British Columbia – its inclusion in the ECCO model reduces the variance of the residuals by up to 17 %. Further analysis indicates that this variance reduction is a robust feature within the time series (see Figure S4).

6. Discussion

[18] We have shown that selfgravitation effects induced by hydrology cause strong deviations from a global uniform distribution of water. Amplitudes are in the order of 5 mm in the open ocean and up to 1 cm along the coast and can be seen as an additional long period ocean tide, with a magnitude comparable to that of the classical luni-solar long period ocean tides [*Wunsch*, 1967].

[19] At the larger scales, the GRACE-based results in Figure 1 are in excellent agreement with the model based results of *Tamisiea et al.* [2010, Figure 3]. Significant differences in the relative deviation from the mean cycle (i.e, after scaling both results by the amplitude of the mean eustatic cycle) are observed near the larger river basins, in particular the Amazon (20–30% between GRACE and GLDAS based estimates), Ganges (30–40%) and Zambezi basins (10–20%), where the hydrological model tends to underestimate the annual land water storage variations, thus reducing the gravitational forcing and solid earth deformation in these regions. As discussed above, the phase difference between the local mass variations and the global mean ocean mass cycle then determines whether the local annual passive sea level cycle will be under- (Ganges) or overestimated (Amazon and Zambezi). Smaller, yet significant, differences are found in the high North, such as near the Gulf of Alaska and Scandinavia. This underlines the added value of the GRACE observations in the computation of passive sea level. Although hydrological mass variations dominate passive sea level variations, a further refinement may be obtained by including the effect of atmospheric induced variations – the second largest component of the global annual water cycle – by means of atmospheric model data [*Tamisiea et al.*, 2010].

[20] Although steric variations and ocean dynamics may be expected to dominate sea-level variability in the majority of the oceans, selfgravitation effects are significant in coastal zones and inclusion of this effect would provide an advancement in ocean modeling. Our comparison between OBP variations from GRACE observations and the ECCO model shows that including selfgravitation effects reduces the residual variance by ~15% in coastal areas at seasonal time scales. Given the large deviations from the global eustatic distribution, numerical ocean models attempting to incorporate the global ocean-land water cycle should consider the implementation of this additional regional forcing mechanism. Furthermore, interannual variations in hydrological loading, e.g., due to ENSO, will cause similar effects as described here. The associated regional variations in relative sea level may affect estimates of global mean sea level change based on tide gauge records, due to uneven sampling of the signal, and should be corrected for where possible.

References

Chambers, D. P., J. Wahr, and R. S. Nerem (2004), Preliminary observations of global ocean mass variations with GRACE, *Geophys. Res. Lett.*, *31*, L13310, doi:10.1029/2004GL020461.

Chambers, D. P., M. E. Tamisiea, R. S. Nerem, and J. C. Ries (2007), Effects of ice melting on GRACE observations of ocean mass trends, *Geophys. Res. Lett.*, *34*, L05610, doi:10.1029/2006GL029171.

Clarke, P. J., D. A. Lavallée, G. Blewitt, T. M. van Dam, and J. M. Wahr (2005), Effect of gravitational consistency and mass conservation on seasonal surface mass loading models, *Geophys. Res. Lett.*, *32*, L08306, doi:10.1029/2005GL022441.

Farrell, W., and J. Clark (1976), On postglacial sea level, *Geophys. J. R. Astron. Soc.*, *46*, 647–667.

Fukumori, I., R. Raghunath, L.-L. Fu, and Y. Chao (1999), Assimilation of TOPEX/Poseidon altimeter data into a global ocean circulation model: How good are the results?, *J. Geophys. Res.*, *104*, 25,647–25,665, doi:10.1029/1999JC900193.

Mitrovica, J. X., M. E. Tamisiea, J. L. Davis, and G. A. Milne (2001), Recent mass balance of polar ice sheets inferred from patterns of global sea-level change, *Nature*, *409*, 1026–1029.

Riva, R. E. M., J. L. Bamber, D. A. Lavallée, and B. Wouters (2010), Sea-level fingerprint of continental water and ice mass change from GRACE, *Geophys. Res. Lett.*, *37*, L19605, doi:10.1029/2010GL044770.

Rodell, M., and P. R. Houser (2004), Updating a land surface model with MODIS-derived snow cover, *J. Hydrometeorol.*, *5*, 1064–1075, doi:10.1175/JHM-395.1.

Rodell, M., et al. (2004), The Global Land Data Assimilation System, *Bull. Am. Meteorol. Soc.*, *85*, 381–394.

Swenson, S., D. Chambers, and J. Wahr (2008), Estimating geocenter variations from a combination of GRACE and ocean model output, *J. Geophys. Res.*, *113*, B08410, doi:10.1029/2007JB005338.

Tamisiea, M. E., E. M. Hill, R. M. Ponte, J. L. Davis, I. Velicogna, and N. T. Vinogradova (2010), Impact of self-attraction and loading on the annual cycle in sea level, *J. Geophys. Res.*, *115*, C07004, doi:10.1029/2009JC005687.

Tapley, B., S. Bettadpur, J. Ries, P. Thompson, and M. Watkins (2004), GRACE measurements of mass variability in the Earth system, *Science*, *305*, 503–505.

Wahr, J., S. Swenson, and I. Velicogna (2006), Accuracy of GRACE mass estimates, *Geophys. Res. Lett.*, *33*, L06401, doi:10.1029/2005GL025305.

Woodward, R. (1888), On the form of and position of mean sea level, *U.S. Geol. Surv. Bull.*, *48*, 87–170.

Wouters, B., and E. J. O. Schrama (2007), Improved accuracy of GRACE gravity solutions through empirical orthogonal function filtering of spherical harmonics, *Geophys. Res. Lett.*, *34*, L23711, doi:10.1029/2007GL032098.

Wunsch, C. (1967), The long-period tides, *Rev. Geophys.*, *5*, 447–475, doi:10.1029/RG005i004p00447.

J. L. Bamber, Bristol Glaciology Centre, School of Geographical Science, University Road, Bristol BS8 1SS, UK.

D. A. Lavallée and R. E. M. Riva, Delft Institute of Earth Observation and Space Systems, Delft University of Technology, PO Box 5058, NL-2600 GB Delft, Netherlands.

B. Wouters, Netherlands Royal Meteorological Institute, Wilhelminalaan 10, NL-3732 GK De Bilt, Netherlands. (bert.wouters@knmi.nl)